Low-Shear Modelled Microgravity Environment Maintains Morphology and Differentiated Functionality of Primary Porcine Hepatocyte Cultures

Original Paper

Cells Tissues Organs

Cells Tissues Organs 2010;192:125–140
DOI: 10.1159/000308893

Accepted: December 26, 2009
Published online: April 15, 2010

Low-Shear Modelled Microgravity Environment Maintains Morphology and Differentiated Functionality of Primary Porcine Hepatocyte Cultures

Leonard J. Nelson[a] Simon W. Walker[b] Peter C. Hayes[a] John N. Plevris[a]

[a]Department of Hepatology, University of Edinburgh, Royal Infirmary of Edinburgh, and [b]Reproductive and Clinical Sciences, The Queen's Medical Research Institute, University of Edinburgh, Edinburgh, UK

Key Words

Differentiation · Integrin · Microgravity · Morphology, functional · Ultrastructure/electron microscopy · Low fluid shear · Polarity · Three-dimensional liver cultures · Three-dimensional hepatocyte culture

Abstract

Hepatocytes cultured in conventional static culture rapidly lose polarity and differentiated function. This could be explained by gravity-induced sedimentation, which prevents formation of complete three-dimensional (3D) cell-cell/cell-matrix interactions and disrupts integrin-mediated signals (including the most abundant hepatic integrin $\alpha_5\beta_1$), important for cellular polarity and differentiation. Cell culture in a low fluid shear modelled microgravity (about 10^{-2} *g*) environment promotes spatial colocation/self-aggregation of dissociated cells and induction of 3D differentiated liver morphology. Previously, we demonstrated the utility of a NASA rotary bioreactor in maintaining key metabolic functions and 3D aggregate formation of high-density primary porcine hepatocyte cultures over 21 days. Using serum-free chemically defined medium, without confounding interactions of exogenous bioscaffolding or bioenhancing surface materials, we investigated features of hepatic cellular polarity and differentiated functionality, including expression of hepatic integrin α_5, as markers of functional morphology. We report here that in the absence of exogenous biomatrix scaffolding, hepatocytes cultured in serum-free chemically defined medium in a microgravity environment rapidly (<24 h)

Abbreviations used in this paper

2D	Two-dimensional
3D	Three-dimensional
AO	Acridine orange
ECM	Extracellular matrix
EGF	Endothelial growth factor
EtBr	Ethidium bromide
FDA	Fluorescein diacetate
HE	Haematoxylin and eosin
HGF	Hepatocyte growth factor
NPC	Non-parenchymal cell
PAS	Periodic acid-Schiff
PPH	Primary porcine hepatocyte
RCCS-HARV	Rotary cell culture system-high aspect ratio vessel
SCB	Sodium cacodylate buffer
SEM	Scanning electron microscopy
TCP	Tissue culture plastic
TEM	Transmission electron microscopy
WE medium	William's E medium

KARGER

Fax +41 61 306 12 34
E-Mail karger@karger.ch
www.karger.com

1422–6405/10/1922–0125$26.00/0

Accessible online at:
www.karger.com/cto

Dr. Leonard J. Nelson
Laboratory Department of Hepatology, University of Edinburgh
Royal Infirmary of Edinburgh, 49 Little France Crescent
Edinburgh EH16 4SB (UK)
Tel. +44 131 242 1631, Fax +44 131 242 1638, E-Mail lenny.nelson@btinternet.com

form macroscopic (2–5 mm), compacted 3D hepatospheroid structures consisting of a shell of glycogen-positive viable cells circumscribing a core of eosinophilic cells. The spheroid shell layers exhibited ultrastructural, morphological and functional features of differentiated, polarized hepatic tissue including strong expression of the integrin α_5 subunit, functional bile canaliculi, albumin synthesis, and fine ultrastructure reminiscent of in vivo hepatic tissue. The low fluid shear microgravity environment may promote tissue-like self-organization of dissociated cells, and offer advantages over spheroids cultured in conventional formats to delineate optimal conditions for enhanced directed tissue self-assembly.

Introduction

Conventional hepatocyte (static) culture on two-dimensional (2D) surfaces such as tissue culture plastic (TCP) or collagen disrupts tissue organization, cell shape and polarity, resulting in retrodifferentiation and loss of hepatic gene expression and function [Berthiaume et al., 1996; Gkretsi et al., 2007; Yamada and Cukierman, 2007]. Three-dimensional (3D) cultures mimic aspects of the in vivo microenvironment, providing another dimension, which favours unconstrained culture system dynamics. External mechanical inputs and cell-adhesive properties dramatically affect integrin ligation, cell contraction and associated intracellular signalling [Griffith and Swartz, 2006]. Partial restoration of cell polarity and differentiated function is achieved in chemically defined media using conventional collagen gel sandwiches or 3D matrices such as Matrigel™ [Berthiaume et al., 1996; Michalopoulos et al., 1999; Tuschl et al., 2009]. In the latter study, it is suggested integrin-mediated reorganization of cell-extracellular matrix (ECM) and cell-cell interactions are involved in hepatocyte differentiation. Interestingly, significant differences in biological functions, including altered cellular proliferation, metabolism, gene expression as well as cell shape and polarity are also observed between tumour cells cultured in 3D compared with 2D monolayers [Feder-Mengus et al., 2008]. Finally, cell-cell and cell-ECM contacts both contribute to the establishment of cell polarity in vivo [Théry et al., 2006], so enabling hepatocytes to respond properly to environmental changes and signals [Gkretsi et al., 2007] whereas hepatocyte dedifferentiation in vitro is an active (reversible) process driven by integrin-associated, focal adhesion kinase-mediated intracellular signaling [Godoy et al., 2009].

Different strategies used to invoke 3D cell culture configurations which recreate aspects of 3D liver tissue organization and appropriate local microenvironment cues include: the formation of hepatocyte spheroids from cell suspensions using spinner flasks, conventional stirred reactors [Martin and Vermette, 2005] and the use of roller bottle cultures with microcarrier-attached hepatocytes [Jauregui et al., 1997] with or without synthetic support structures [Liu Tsang et al., 2007]. Heterotypic cocultures of rat hepatocytes and non-parenchymal cells (NPCs) in collagen-coated roller bottle cultures yielded structured tissue-like formations bearing resemblance to hepatic histological organization [Michalopoulos et al., 2001]. Hepatocyte aggregation in these systems contributes to 3D cellular arrangements and enhanced cell-cell interactions which have been reported to prolong and improve hepatocyte function in vitro compared with traditional 2D cultures [Lazar et al., 1995a, b; Auth and Ichihara, 1998; Tuschl et al., 2009]. For example, a significant increase in albumin synthesis can be induced in engineered liver tissue by hepatocyte aggregation [Parsons-Wingerter and Saltzman, 1993; Kim and Mooney, 1998; Nahmias et al., 2007]. In these dynamic culture modalities, however, physical forces of high-shear stress, which damage the cells by fluid shear forces, rotationary impeller impacts and gravity-induced sedimentation, may hinder proper tissue-specific differentiation [Spaulding et al., 1993; Unsworth and Lelkes, 1998; Nahmias et al., 2007].

To offset the high-shear forces, NASA developed a novel rotating wall vessel bioreactor: the rotary cell culture system-high aspect ratio vessel (RCCS-HARV) – which promotes growth of fastidious, delicate cells in a simulated, or low-shear modelled microgravity environment [Navran, 2008]. Human liver, cartilage, bone marrow, skin explants and various cell lines have been successfully cultured in the RCCS-HARVinto macroscopic, differentiated, tissue-like 3D constructs [Becker et al., 1993; Goodwin et al., 1993; Jessup et al., 1993; Spaulding et al., 1993; Navran, 2008]. The HARV facilitates microgravity (about 10^{-2} *g*) by promoting randomized angular gravitational vectors on the growing aggregate, thus creating a free-fall (quasi-stationary) rotation of the cell aggregate(s) around a horizontal axis within the vessel. The resultant low fluid-shear mass transfer of nutrients and waste products with high oxygenation promotes close apposition (spatial colocation) of single-cell suspensions moving along with the fluid in the HARV, resulting in microgravity-induced, 3D cell formations [Botta et al., 2006; Navran, 2008; Mazzoleni et al., 2009]. However, the mechanisms responsible for this self-assembly of cells to

aggregate remain to be established [Khaoustov et al., 1999].

Preferential aggregation in microgravity may not only enhance cell-cell interactions, differentiated function and cell polarity, but may also induce tissue-specific upregulation of cell adhesion molecules (such as integrins and cadherins), ECM proteins and their respective integrin receptors [Unsworth and Lelkes, 1998]. Recent microarray studies show upregulation of cell adhesion molecules in spheroid cultures of HepG2 cells in microgravity [Chang and Hughes-Fulford, 2009] and rat hepatocyte spheroids in a novel spheroid rocker dish [Brophy et al., 2009]. ECM geometry, in concert with mechanical stress mediated by adhesive cell-cell and cell-ECM interactions, modulates and maintains structural and differentiated functional features of hepatocytes in vivo, such as expression of cell surface adhesion molecules, albumin production and urea synthesis [Berthiaume et al., 1996; Bhatia et al., 1998a, b, 1999; Griffith and Swartz, 2006; Nahmias et al., 2007]. Such regulatory effects of ECM are often mediated by integrins, which comprise a large family of cell surface receptors that attach cells to ECM proteins and mediate mechanical and chemical signals arising from ECM. For example, the most abundant hepatocyte integrin, the fibronectin receptor $\alpha_5\beta_1$, is thought to be involved in the coordinated control of cell shape, growth and survival, important for the establishment and maintenance of tissue architecture [Stamatoglou et al., 1990; Stamatoglou and Hughes, 1994; Giancotti and Ruoslahti, 1999]. Indeed, antibodies blocking the binding of integrin β_1 subunits to collagen in collagen-sandwiched hepatocyte cultures resulted in significant alterations in hepatic morphogenesis, cell polarity and differentiated function [Moghe et al., 1997]. Using time lapse microscopy, Peshwa et al. [1996] revealed that cell movement and reorganization were involved in spheroid formation, implicating a mechanistic role for integrins. In fact, integrin bridging between the cellular cytoskeleton and ECM components allows cells to exert force on their environment, critical for many cellular processes including efficient cell movement [Holly et al., 2000]. Integrins likely play an important role in the differentiation of the epithelial and endothelial cell populations of the liver [Couvelard, 1998]. Indeed, via integrins, cells can sense dimensionality and other physical and biochemical properties of the ECM [Larsen et al., 2006].

Given the importance of these factors in the expression of cell polarity, liver-specific functions and histological architecture, the present study was designed to investigate the hypothesis that microgravity hepatic cultures maintained 3D aggregate formations, cellular polarity and differentiated functionality for a predetermined period of 12 days. Furthermore, using chemically defined medium, without confounding interactions of exogenous bio-scaffolding or bio-enhancing surface materials, the expression of integrin α_5, a marker of hepatic differentiation and structural integrity, was investigated.

Materials and Methods

Reagents

All reagents used including William's E (WE) medium, supplements, buffers and fluorescein diacetate (FDA) were obtained from Sigma. The primary antibody, polyclonal anti-integrin α_5 (raised in goat) was purchased from Insight Biotechnology (Middlesex, UK). The secondary antibody, indodicarbocyanine, Cy3™-conjugated donkey anti-goat IgG and normal donkey serum (60 mg/ml) were supplied by Jackson Immunoresearch (West Grove, Pa., USA).

Hepatocyte Isolation and Culture

Hepatocytes were isolated from weanling piglets (<15 kg) using our ex vivo collagenase perfusion method [Nelson et al., 2000]. As judged by the size (<10 μm in diameter) and morphology (non-polygonal or stellate) of the NPCs, the NPC fraction was <5%. To verify cell viability following microgravity culture, a spheroid sample cultured for 12 days in serum-free chemically defined WE medium in the RCCS-HARV was dispersed by gentle pipetting and transferred to TCP dishes and cultured for 2 days in the same medium. Otherwise, hepatocytes were cultured as described in Nelson et al. [2000].

Hepatocyte Culture in Simulated Microgravity

Primary porcine hepatocytes (PPHs) were cultured in simulated microgravity using the RCCS-HARV. Microgravity conditions were simulated using two RCCS-HARV configurations: (1) 55-ml capacity single-station RCCS-HARV and (2) 50-ml capacity, four-station RCCS-HARV. Preliminary work: in order to optimize the consistent formation of cell aggregates in simulated microgravity empirically, cells were seeded (day 0) in the 50-ml capacity HARVs (Cellon-Sarl, Luxembourg) at densities of 0.25, 0.5, 1.0 or 2×10^6 viable cells per millilitre of WE medium at 37°C. High seeding densities of 2×10^6 viable cells per millilitre gave the most consistent simulated microgravity culture of aggregates in free-fall rotation as defined above, and were used for all subsequent experiments. The HARV was connected to the horizontally rotating axle of the RCCS, which pumped incubator gas via a central aperture, across a silicon rubber, semi-permeable gas exchange membrane within the HARV. The RCCS-HARV assembly was placed in a humidified incubator under a 95% air:5% CO_2 atmosphere. On the next day (day 1), aggregated cells were allowed to sediment, the HARV was aspirated, and pre-warmed, fresh medium added, and subsequently changed every 2 days. The optimal rotational speed of the HARV was determined by adjusting the RCCS rotational speed such that the aggregate(s) maintained a free-fall, quasi-stationary orbit within the culture vessel. The rotational speed varied according to both aggregate size and

the corresponding sedimentation coefficient. However, by day 6 of culture, rotational speed was set between 10 and 15 rpm. For changes of WE medium, a 0.5-cm fill port and a suction aspirator were used. Medium was replenished on days 1 and 2, and every 2 days thereafter. When changing the medium, the cells were covered by a small amount of medium to minimize cell damage. Medium samples were taken at the time points indicated via a sterile syringe attached to one of the HARV luer-lock syringe ports and stored at –80°C until analysis.

Morphology

Histology of Cell Aggregates

On days 2, 6, and 12 for HARV-grown aggregates, cell samples were removed and fixed in 3% formaldehyde/0.1 M cacodylate buffer. The fixative was aspirated and the cells washed with PBS; cell aggregates were resuspended in 100 μl of molten agarose for ease of handling. Histological staining was performed using haematoxylin and eosin (HE) to identify hepatocyte nuclei and cytoplasm, respectively. Periodic acid-Schiff (PAS) reagent was used to detect the presence of glycogen. Subsequent sample processing and staining were performed using standard techniques. Morphology was recorded by photomicrography using an inverted microscope (Zeiss, Germany) under transmitted light for each culture modality at each time point.

Scanning Electron Microscopy

Freshly isolated hepatocytes and cell aggregates were taken from the RCCS-HARV on days 6 and 12 and then processed using standard techniques. Briefly, samples were washed in HBSS buffer and subjected to low-speed centrifugation (20 *g*) for 5 min. Cell samples were fixed in 3% glutaraldehyde in 0.1 M sodium cacodylate buffer (SCB) at pH 7.4 for at least 3 h. Following washing in 0.1 M SCB, samples were post-fixed with 1% osmium tetroxide in 0.1 M SCB for 2 h and washed in distilled water. Following dehydration (3 times) in a graded series of acetone (50, 70, 90 and 100%), cells were subjected to critical-point drying with CO_2 in a Poleron E3000 SII critical-point dryer. For conductive coating, samples were sputter-coated with 20 nm gold/palladium (60/40) in an Emscope sputter coater. Finally cell aggregates were viewed in a Philips 505 scanning electron microscope.

Transmission Electron Microscopy

Cell aggregates taken from the RCCS-HARV on days 6 and 12 were washed in HBSS buffer and subjected to low-speed centrifugation (20 g) for 5 min. Cell samples were fixed in 3% glutaraldehyde in 0.1 M SCB and processed using standard techniques.

Confocal Microscopy

The following protocol was modified from Stamatoglou et al. [1990]. Aggregate samples from the HARV on days 3 and 12 were fixed in formal saline (4% formaldehyde/4% paraformaldehyde/0.4 M sucrose) for 2 h at room temperature and then washed in PBS with 0.5% Triton-X for 30 min. RCCS aggregates were transferred to 1.5-ml Eppendorf tubes for three 20-min washes with 1% donkey serum albumin in PBS on a Spiramix roller bottle tray. For static cultures, slides were similarly treated and gently shaken on an orbital shaker. Titration of the polyclonal anti-α_5 integrin (goat) primary antibody resulted in an optimal concentration of 1:20 for indirect immuno-fluorescence. Fifty microlitres of primary antibody were added to samples for 1 h at room temperature. After the primary antibody incubation, the cells were washed three times in PBS for 20 min before addition of the secondary antibody. The Cy3-conjugated donkey anti-goat IgG secondary antibody was used at a dilution of 1:20 (in 1% donkey serum albumin/PBS), 50 μl added and incubated for 20 min at room temperature. Unbound antibody was removed by three 20-min washes with 1% normal donkey serum in PBS. RCCS aggregate samples were mounted in 50:50 glycerol:PBS in wells made by strips of coverslip on standard glass slides. The wells were sealed with nail varnish to prevent leakage. For 2D cultures: the Lab-Tek™ glass chamber slide cultures were mounted in 50:50 glycerol:PBS and covered with a glass coverslip and sealed as above. Cells were viewed using a Leica TCSNT confocal microscope system (Heidelberg, Germany) with a 10× objective lens or a 63× water-corrected lens with the argon-krypton laser set at λ_{568} nm. Images were recorded on computer and stored on a CD for future analysis. (1) Negative controls: cells were treated as above except that the primary antibodies were omitted; (2) positive controls: fresh human and pig liver samples were homogenized in SDS/PBS and dot blot analysis was performed of cell lysates using the above primary antibody and an HRP-conjugated donkey anti-goat IgG secondary antibody revealing high (human) and moderate (pig) levels of cross-reactivity (performed courtesy of Dr. A.F. Howie, Department of Clinical Biochemistry, University of Edinburgh, UK).

Vital Staining using Acridine Orange/Ethidium Bromide Fluorescent Dye

To assess cell viability, fresh HARV-cultured cell aggregate samples were taken on day 12 and, following cytospin, 5 μl (100 μg/ml) of the fluorescent dyes, acridine orange (AO)/ethidium bromide (EtBr) in WE medium was added for 2 min at room temperature. Viable (apple green nuclei) and non-viable cells (yellow/orange nuclei) were visualized using confocal microscopy (see below) and photographed.

Functional Assays

Immunodetection of Albumin in PPH Culture Supernatants

The presence of albumin was confirmed in microgravity cultures on days 6 and 12 by dot blot analysis followed by densitometry/chemiluminescent assay. Briefly, duplicate samples of culture supernatants were taken on days 6 and 12, and 5 μl blotted onto nitrocellulose strips and dried with a hairdryer. This was repeated with a pig albumin standard (1 mg/ml) made up in WE medium at a range of concentrations (0–200 μg/ml). The nitrocellulose strips were washed three times for 5 min in 0.5% (v/v) Tween-20 PBS solution and incubated for 2 h on a rotary shaker at room temperature with Pierce™ blocking buffer to prevent non-specific binding. The first anti-human albumin antibody (rabbit) was titrated to 1:2,000 in the PBS/Tween-20 solution with 3% (w/v) dried milk (Marvel) and incubated for 1 h at room temperature on a rotary shaker. This was followed by five 6-min washing steps in the 0.5% PBS/Tween-20 solution. The second (first) antibody (anti-rabbit HRP-conjugated) was titrated to 1:20,000 and incubated for 1 h as above, and the washing steps repeated. Controls: (1) albumin standard without the first antibody and (2) test media (never-seen cells) were similarly treated. A chemiluminescent agent (Supersignal, Pierce™) was added to the nitrocellulose strips (0.75 ml per strip) for 5 min, wrapped in cling-film and either exposed to photographic film (Kodak™

Omat Film) for 3–4 min or subjected to densitometry using a Bio-rad™ (phosphoimager) image analysis system.

Fluorescein Diacetate Metabolism of Cultured PPHs

The bile acid analogue FDA used to assess functional metabolism of day-12 cultures was analysed to assess bile canalicular function. Eighty microlitres of FDA was added for 30 min to aggregates transferred to a 10-ml capacity RCCS placed in a CO_2 incubator at 37°C according to Mitaka et al. [1999]. Cells were subsequently rinsed three times with warm PBS following brief centrifugation at low speed (25 *g*), placed on glass microscope slides and photographed using a Leitz Wetzlar Ortholux II fluorescent microscope with a 25× water immersion lense.

Results

Cell Isolation, Viability and Yield

The hepatocytes were isolated using our ex vivo method [Nelson et al., 2000]. For these experiments, cell viability was 87 ± 5% with a yield of $2.2 \pm 0.8 \times 10^{10}$ cells from piglets weighing 12 ± 1 kg (n = 5).

Morphology of Freshly Isolated Primary Porcine Liver Tissue

Histology and Ultrastructure

Figure 1a shows a phase-contrast image of freshly isolated hepatocytes with bright cytoplasms, sharply defined borders with a round or polygonal shape; cells stained with PAS glycogen and counter-stained with HE show eosinophilic cytoplasms and distinct nuclei (fig. 1b). For subsequent comparison with PPH cultures grown in microgravity, we examined the ultrastructure of fresh liver tissue and isolated hepatocytes, which revealed common fine structural features. Scanning electron microscopy (SEM): following low-speed centrifugation, single cells and typical PPH 5- to 20-cell clusters appeared as a densely packed arrangement at both low (fig. 1c) and higher magnification (fig. 1d). Note the presence of numerous microvilli on the surface of hepatocytes, indicative of highly differentiated cells. Transmission electron microscopy (TEM) confirmed common fine structural features: round nuclei with nucleoli and well-defined plasma and nuclear membranes (fig. 1e); abundant mitochondria and granular endoplasmic reticulum interspersed between the mitochondria; smooth endoplasmic reticulum and Golgi apparatus; numerous dense glycogen β-particles and rosettes (α-particles) (fig. 1f, g) between smooth endoplasmic reticulum and in close proximity to mitochondria, peroxisomes and lysosomes. Bile canaliculus-like structures are evident in both fresh liver tissue (fig. 1f, h) and in isolated hepatocytes (fig. 1i). It is noteworthy that following collagenase digestion of pig liver, the cell clusters have a high content of sugar residues (glycocalyx) on the hepatocyte cell surface, which may enhance cell-cell adhesion in 3D culture [unpublished data]. Carbohydrate-based domains may also improve on hepatocyte adhesion. For example, incorporation of galactose-derived sugars onto various surfaces has been reported to confer hepatocyte adhesion and spreading via an asialoglycoprotein receptor and may offer an alternative to or work in conjunction with adhesion peptide moieties [Liu Tsang et al., 2007].

Morphology of Hepatocytes Cultured in Modelled Microgravity Environment

Histology and Ultrastructure: Day 6

Figure 2 shows hepatocytes cultured for 6 days in serum-free chemically defined WE medium in simulated microgravity (about 10^{-2} *g*) formed spheroidal cell aggregates (2–5 mm in diameter) as assessed using a graduated eyepiece graticule under transmitted light. A transverse section (stained with PAS/HE) of a HARV-cultured cell spheroid aggregate shows a distinctive PAS-positive rim of apparently viable cells, some 8–10 cells in depth (about 250 μm) with large round nuclei circumscribing a (hypoxia-induced) necrotic/apoptotic core as evidenced by condensed nuclei and cell degeneration (fig. 2a). These observations suggest that (biomatrix-free) large spheroid cultures have perturbed mass transport and O_2 diffusion limitations, confirming a recent study [Curcio et al., 2007]. SEMs of cell aggregates: figure 2b, c shows rounded hepatocytes organized as tight clusters suggesting extensive cell-cell contacts; note the presence of microvilli on the surface of hepatocytes (closed arrows in fig. 2b, c). TEM: figure 2d shows a binucleate hepatocyte with

Abbreviations used in figures 1–5

Bc	Bile canaliculus-like channels
G	Electron-dense glycogen particle
Ga	Golgi apparatus
ger	Granular endoplasmic reticulum
H	Hepatocyte
L	Lysosome
Mt	Mitochondrion
n	Necrotic/apoptotic core
N	Nucleus
Nm	Nuclear membrane
Nu	Nucleolus
P	Peroxisome
Pm	Plasma membrane

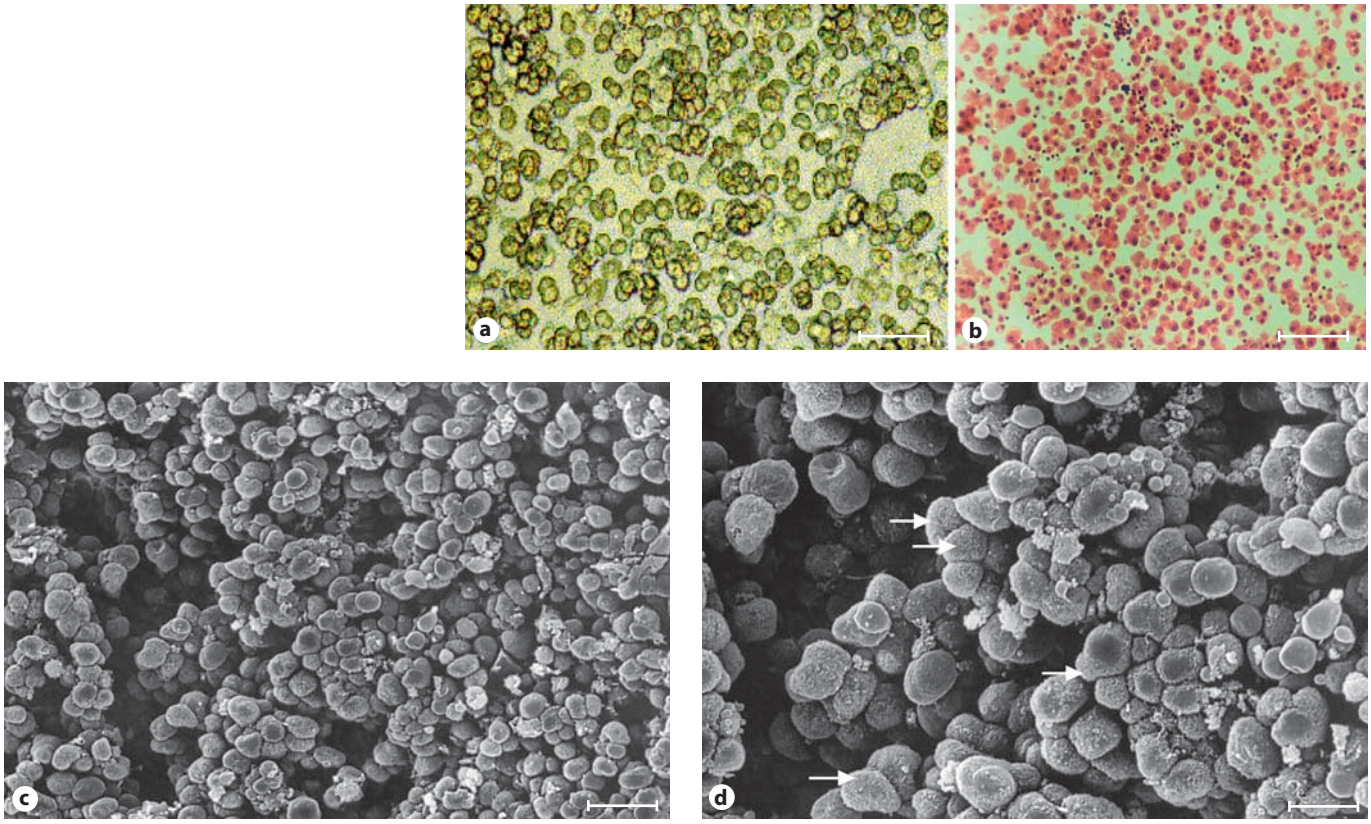

Fig. 1. Gross morphology and ultrastructure of freshly isolated PPHs and fresh liver tissue. **a** Fresh cell suspension just prior to inoculation into the HARV; hepatocytes show bright cytoplasms, sharply defined borders with a round or polygonal shape (bar 100 μm). **b** Cells stained with PAS glycogen stain and counterstained with HE show eosinophilic cytoplasms and distinct nuclei (bar 100 μm). **c**, **d** SEM: following low-speed centrifugation, single cells and 5–20 cell clusters appeared as densely packed arrangements at both low (**c** bar 50 μm) and higher magnification (**d** bar 25 μm). Note the presence of numerous microvilli on the surface of hepatocytes (white arrows in **d**).

prominent round nuclei with nucleoli, abundant mitochondria and granular endoplasmic reticulum; interspersed between the mitochondria are numerous electron-dense glycogen particles; figure 2e shows several hepatocytes whose borders are separated by canaliculus-like channels with characteristic microvillous processes delimited by tight junctions – evidence of polarized epithelial cells [Decaens et al., 2008], and prominent granular endoplasmic reticulum present in the cytoplasm; figure 2f shows part of a nucleus in close proximity to granular endoplasmic reticulum, adjacent mitochondria and glycogen particles.

Histology and Ultrastructure: Day 12

Figure 3 shows that overall morphology of 12-day-old HARV cultures is similar to that seen on day 6 (fig. 2). Viable, PAS-positive cells are present, suggesting that the hepatocytes are differentiated and are producing and storing glucose as glycogen (fig. 3a). SEM: figure 3b shows tightly packed cells organized as an ellipsoidal (oblate spheroid), compact structure with more loosely associated rounded parenchymal cells present on the aggregate surface; at higher magnification (fig. 3c), the smooth appearance on the aggregate surface may be indicative of the compact morphology and the presence of NPCs. Note the presence of microvilli on the surface of hepatocytes. Large ellipsoid-type cell aggregates (about 1,500 × 3,500 μm) were most commonly observed in day-12 cultures; however, the inner cell core, without biomatrix support, may exceed optimal mass transport of nutrients (particularly O_2 diffusion) in spheroid cultures >200–300 μm [Curcio et al., 2007]. However, a recent analysis [Kwon et al., 2008] proposes that stringent control of the rotational speed of microgravity culture vessels

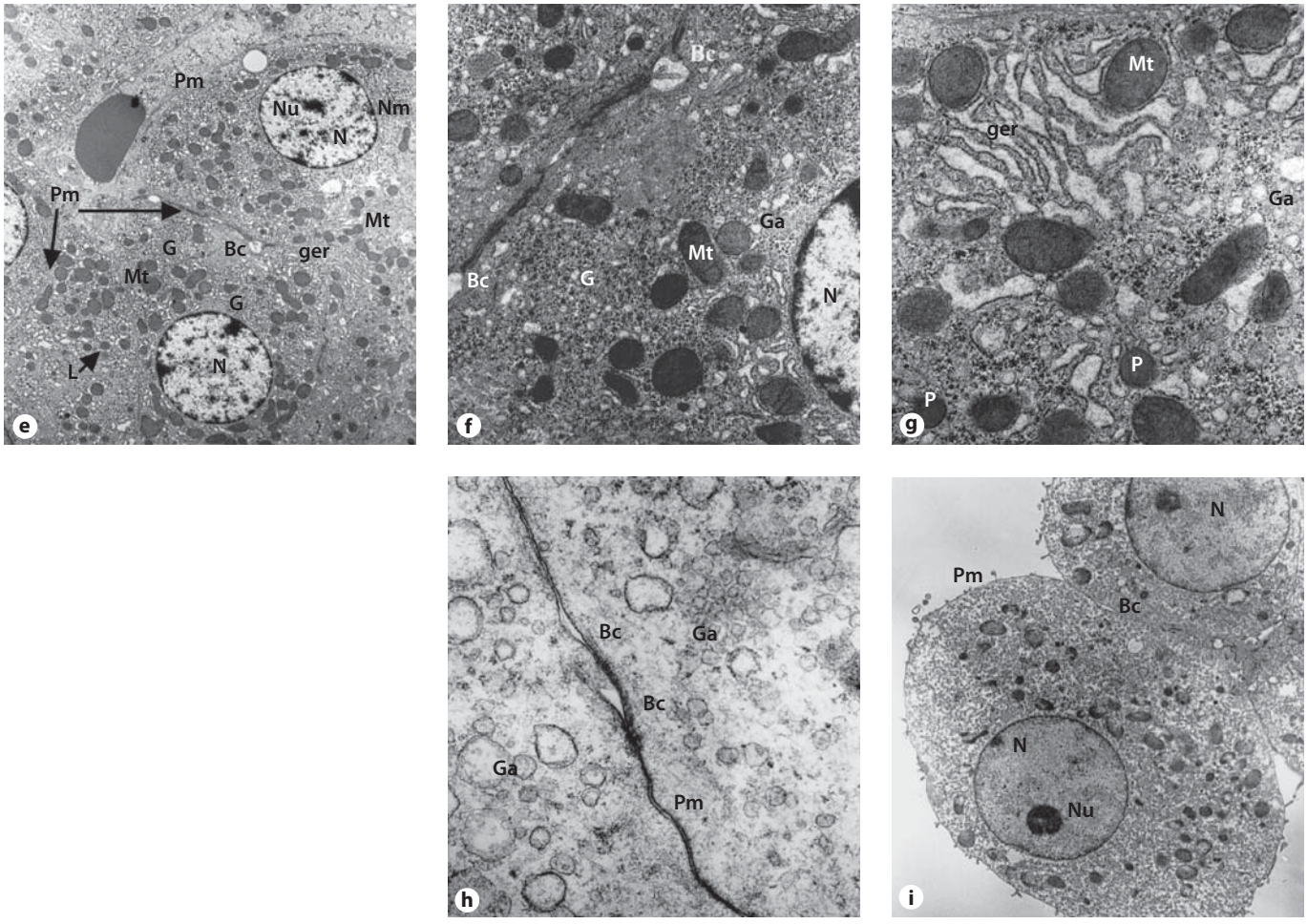

Fig. 1. e–i TEM of fresh liver tissue and isolated hepatocytes shows common fine structural features. Round nuclei with nucleoli and well-defined plasma and nuclear membranes (**e** ×3,800); abundant mitochondria and granular endoplasmic reticulum interspersed between the mitochondria; smooth endoplasmic reticulum and Golgi apparatus; numerous dense glycogen β-particles and rosettes (α-particles) (**f** ×10,000, **g** ×17,000) between smooth endoplasmic reticulum and in close proximity to mitochondria, peroxisomes and lysosomes. Bile canaliculus-like structures are evident in both fresh liver tissue (**f**, **h** ×28,000) and in isolated hepatocytes (**i** ×3,800).

can dramatically improve zonal mean [O_2] via increased fluid convection. TEM micrographs: figure 3d shows bile canaliculus-like channels with characteristic microvillous processes between several juxtaposed polygonal hepatocytes. Ultrastructural features of fresh liver tissue (fig. 1) are evident, although there is an asymmetric cytoplasmic distribution of granular endoplasmic reticulum, mitochondria and other organelles; interspersed between the mitochondria are numerous electron-dense glycogen particles. A possible NPC is resident in the centre right of this image. Figure 3e shows part of the hepatocyte nucleus in close proximity to mitochondria and lysosomes and adjacent glycogen particles. Figure 3f is a high-magnification image of a bile canaliculus showing microvillous processes and adjacent Golgi apparatus.

Parameters of Cell Viability and Functional Polarity in Day-12 Microgravity Cultures

Figure 4 shows confocal imaging. Figure 4a shows part of a cell aggregate (broken off from a larger aggregate during the sampling process), stained with the fluorescent dyes AO/EtBr: viable cells stain apple green, whereas non-viable/apoptotic cells stain orange-yellow. This demonstrates that at least part of the outer layer of HARV-cultured cellular aggregates remain viable up to culture day 12 in simulated microgravity. Figure 4b shows green FDA fluo-

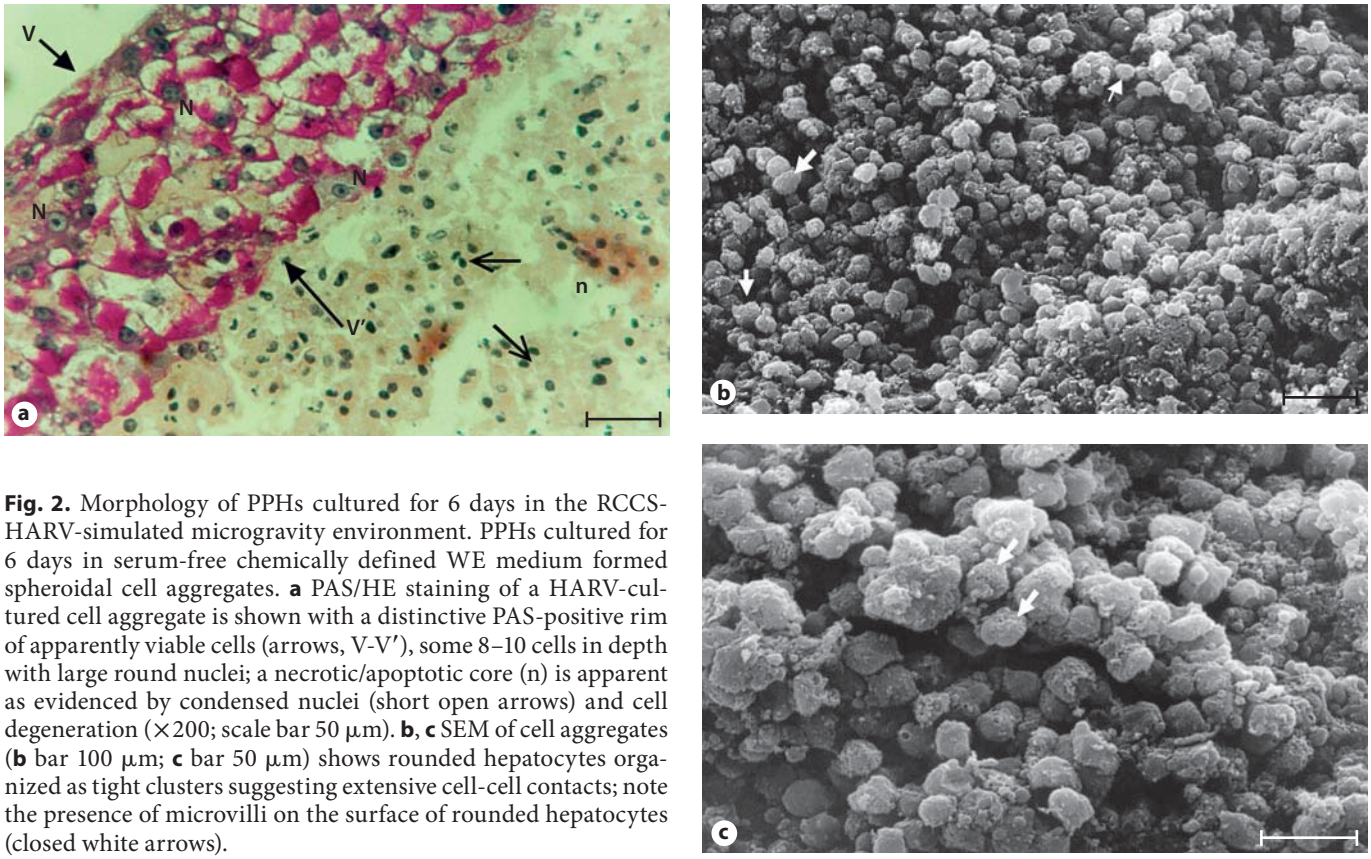

Fig. 2. Morphology of PPHs cultured for 6 days in the RCCS-HARV-simulated microgravity environment. PPHs cultured for 6 days in serum-free chemically defined WE medium formed spheroidal cell aggregates. **a** PAS/HE staining of a HARV-cultured cell aggregate is shown with a distinctive PAS-positive rim of apparently viable cells (arrows, V-V′), some 8–10 cells in depth with large round nuclei; a necrotic/apoptotic core (n) is apparent as evidenced by condensed nuclei (short open arrows) and cell degeneration (×200; scale bar 50 μm). **b**, **c** SEM of cell aggregates (**b** bar 100 μm; **c** bar 50 μm) shows rounded hepatocytes organized as tight clusters suggesting extensive cell-cell contacts; note the presence of microvilli on the surface of rounded hepatocytes (closed white arrows).

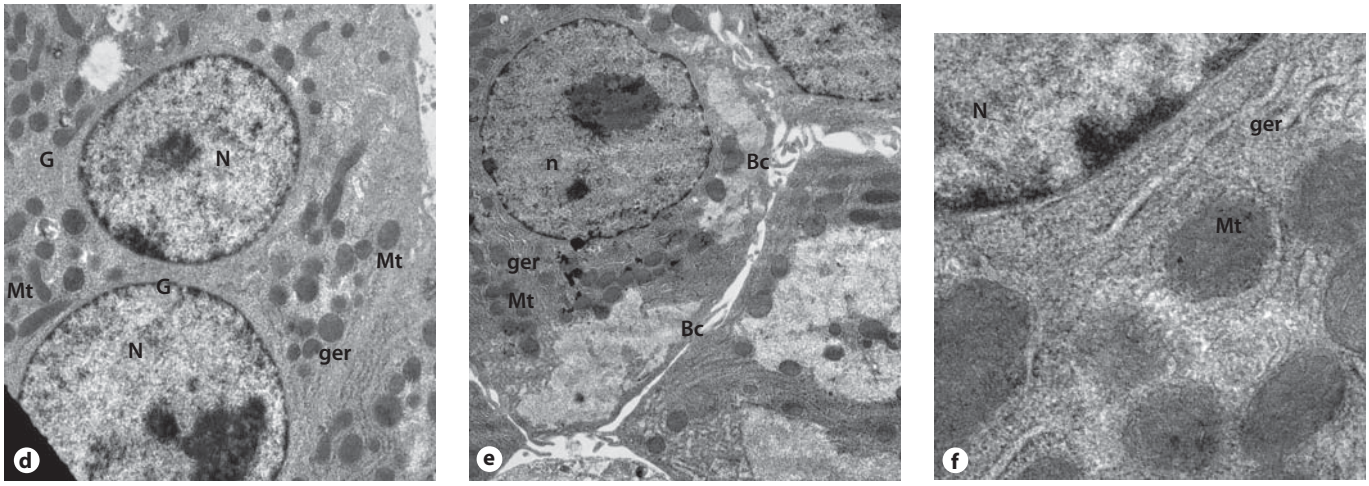

Fig. 2 d–f TEM. **d** Binucleate hepatocyte with prominent round nuclei with nucleoli, abundant mitochondria and granular endoplasmic reticulum; interspersed between the mitochondria are numerous electron-dense glycogen particles (×8,000). **e** Several hepatocytes whose borders are separated by canaliculus-like channels with characteristic microvillous processes delimited by tight junctions; and prominent granular endoplasmic reticulum present in the cytoplasm (×6,300). **f** Part of a nucleus (top left) in close proximity to granular endoplasmic reticulum, adjacent mitochondria and glycogen particles (×45,000).

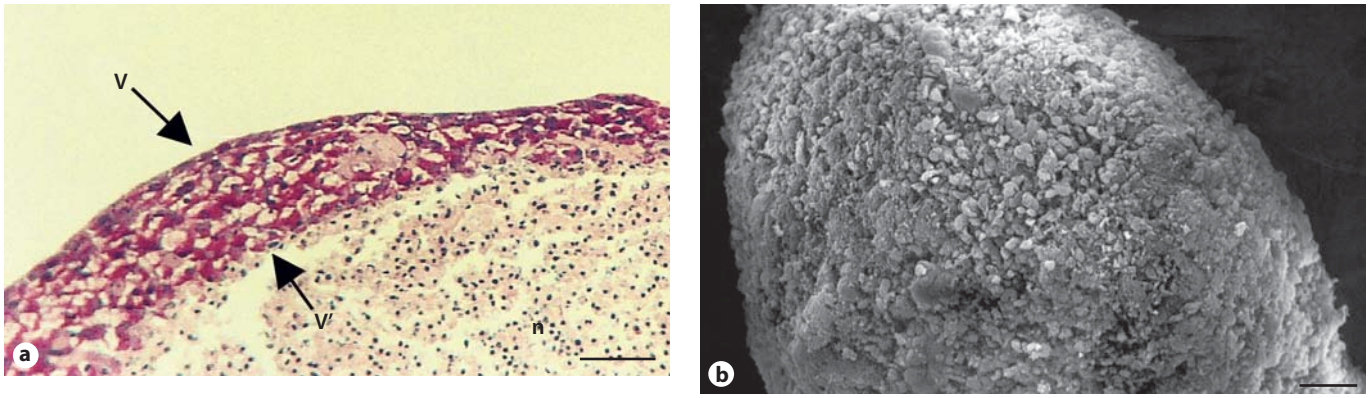

Fig. 3. Morphology of PPHs cultured for 12 days in the RCCS-HARV-simulated microgravity environment. Representative photographs showing morphology of PPH aggregates cultured for 12 days in the HARV. **a**, **b** Photographs of HARV cultures (**a** bar 100 μm; **b** bar 50 μm). Cells were stained with PAS glycogen stain and counterstained with HE. Morphology of 12-day-old HARV cultures is very similar to that seen on day 6 (fig. 2). Note the rim of PAS-positive hepatocytes in **a** (V-V′) with a central core of eosinophilic-rich/necrotic cells. **b**, **c** SEM. **b** Tightly packed arrangement of cells organized as an ellipsoidal, compact structure with more loosely associated rounded parenchymal cells present on the aggregate surface (bar 100 μm). **c** The smooth appearance on the aggregate surface at higher magnification (open arrow) may be indicative of the compact morphology and the presence of NPCs. Note the presence of microvilli on the surface of hepatocytes (closed white arrows) (bar 50 μm).

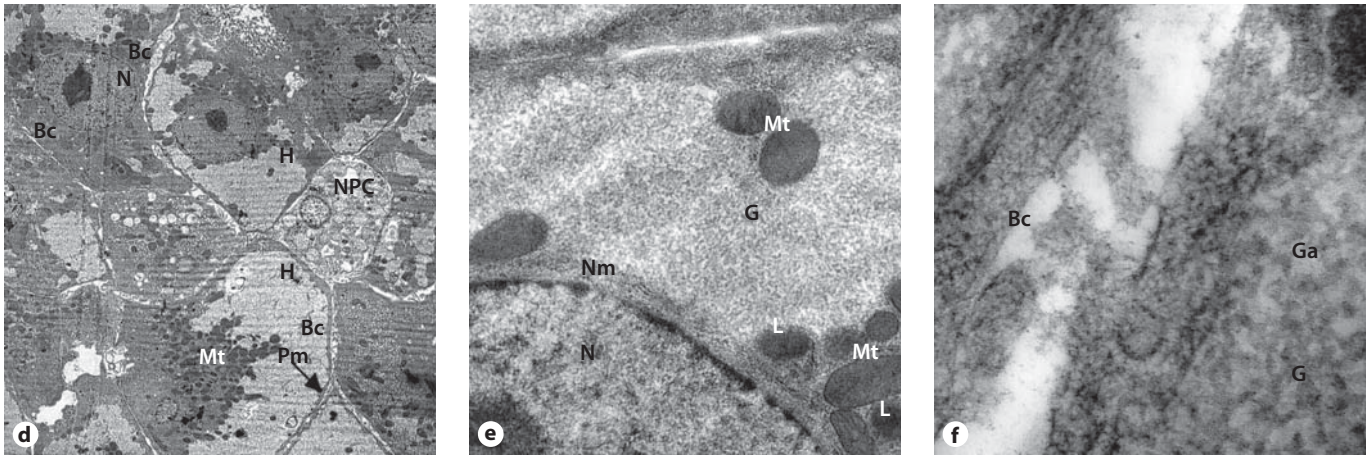

Fig. 3 d–f TEM. **d** Bile canaliculus-like channels with characteristic microvillous processes between several juxtaposed polygonal hepatocytes. Ultrastructural features of fresh liver tissue are evident, although there is an asymmetric cytoplasmic distribution of granular endoplasmic reticulum, mitochondria and other organelles; interspersed between the mitochondria are numerous electron-dense glycogen particles. A possible NPC is resident in the centre right of this image (×1,800). **e** Part of the hepatocyte nucleus (lower left) in close proximity to mitochondria and lysosomes and adjacent glycogen particles (×17,000). **f** High-magnification image (×75,000) of a bile canaliculus showing microvillous processes and an adjacent Golgi apparatus.

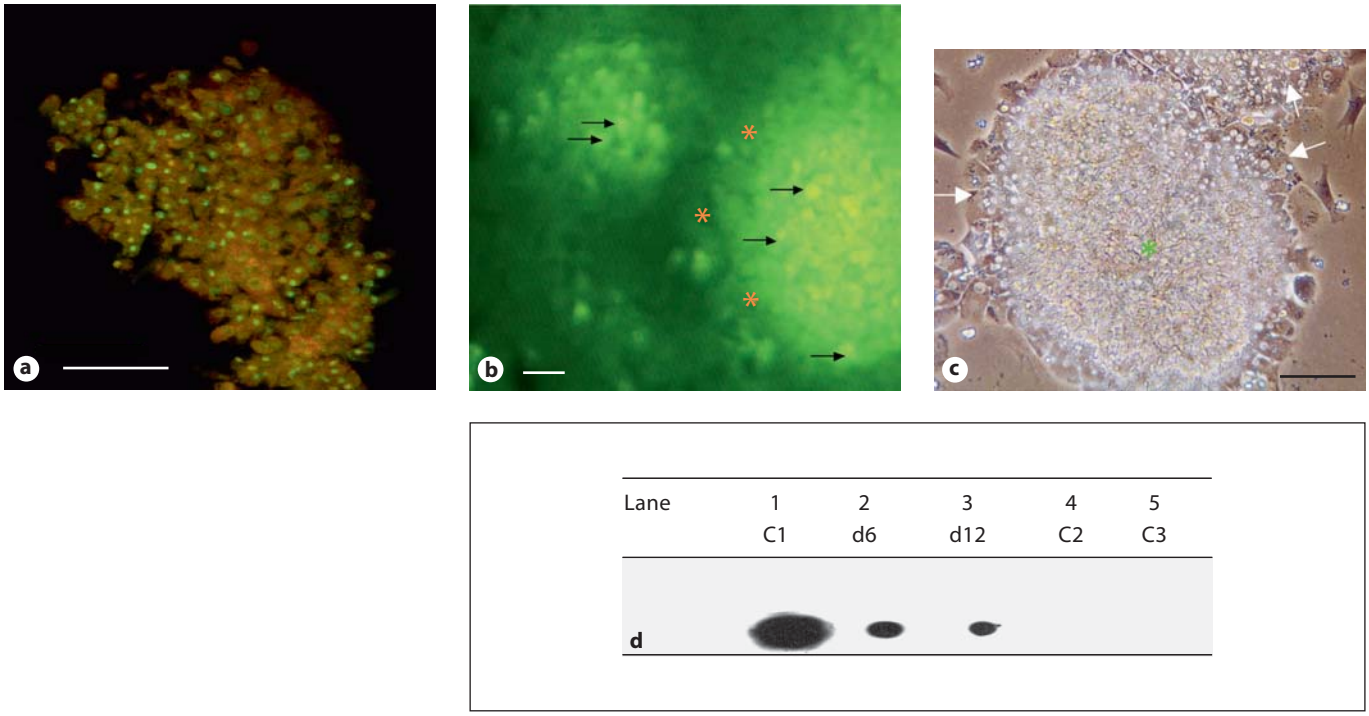

Fig. 4. Morphological and functional parameters showing cell aggregate viability and functional polarity of PPHs cultured for 12 days in the RCCS-HARV modeled microgravity environment. **a–c** Laser scanning confocal imaging. **a** Staining of viable (apple green) and non-viable (diffuse orange-yellow) hepatocytes in the aggregate cultures. Cell aggregates were stained with 2 μl (100 μg/ml) of the fluorescent dyes, AO/EtBr (bar 100 μm). **b** The fluorescent bile acid analogue FDA was used to assess bile canalicular functional metabolism of PPH spheroid cultures (bar 50 μm); FDA is actively taken up across bile canalicular membranes and, following deacetylation, the bright green fluorescent product (arrows) is formed, so confirming the presence of functional bile canaliculi. Strong staining of the compact spheroid surface is evident with little demarcation between individual, adjacent cells. Hepatocyte nuclei (orange asterisks) are just visible in cells on the aggregate periphery. **c** To verify spheroid viability following the cellular stress associated with cell attachment to uncoated TCP, a spheroid sample pre-cultured for 12 days in serum-free chemically defined WE medium in the HARV was dispersed by gentle pipetting and transferred to TCP dishes and cultured for 2 days in the same medium (bar 100 μm). Fragments of the spheroid (asterisk) readily attached to the dish surface and formed hepatocyte monolayers with highly refractile borders radiating from the cell aggregate base (white arrows) after 2 days of culture. **d** Synthesis of albumin was confirmed on days 6 and 12 by dot blot immunodetection. Lane 1, C1: purified pig albumin control (25 μg/ml); lane 2, d6: PPH culture, day 6; lane 3, d12: PPH culture, day 12; lane 4, C2: WE medium (never-seen cells); lane 5, C3: no first antibody added.

rescent staining of two small cell aggregates (broken off from a larger spheroid during preparation). Strong staining of the compact spheroid surface is evident with little demarcation between individual adjacent cells. Hepatocyte nuclei are just visible in cells on the aggregate periphery. Uptake and metabolism of FDA is considered a good marker of functional polarity and canalicular function; however, excretion into the bile canaliculus-like channels could not be resolved. The intensity of fluorescence has also been shown to correlate with cell viability and hepatic-specific function [Nyberg et al., 1993]. To verify cell viability by cell attachment to TCP dishes, a spheroid sample cultured for 12 days in serum-free chemically defined WE medium in the RCCS-HARV, was dispersed by gentle pipetting and transferred to TCP dishes and cultured for 2 days in the same medium. Figure 4c shows a fragment of the spheroid which readily attached to the dish surface and formed hepatocyte monolayers, radiating from the cell aggregate base after 2 days of culture. Synthesis of albumin was confirmed up to day 12 as shown in figure 4d by immunodetection using dot blot analysis.

Integrin α_5 Expresssion

Expression of Integrin α_5 in Freshly Isolated PPHs

Figure 5 shows the expression of the ECM (fibronectin) counterreceptor, integrin α_5 subunit, on a single he-

patocyte (fig. 5a) and a hepatocyte doublet (fig. 5b). Hepatocytes were placed in fixative and processed for indirect immunofluorescent staining only 2 h following the initial isolation step, suggesting cell surface integrins are not degraded in this time frame. Noteworthy is the distinct clustering pattern of integrin α_5, reminiscent of the configuration adopted at focal adhesion complexes in native liver in vivo [Hynes, 2002].

Hepatocytes Cultured in Simulated Microgravity Environment Days 3 and 12

Since integrins mediate dynamic adhesive cell-cell and cell-ECM interactions that regulate a wide variety of dynamic cellular processes, such as cell migration, phagocytosis and growth and development [Hynes, 2002; Arnaout et al., 2007], we sought to establish whether hepatocytes cultured in microgravity conditions showed evidence of the most abundant liver cell adhesion protein, integrin α_5. Figure 5c, e provide compelling evidence of integrin α_5 expression in day-3 and day-12 microgravity cultures; with strong fluorescent staining on cell aggregate surfaces (fig. 5d) and the appearance of integrin 'hotspots' (fig. 5e) on the surfaces of aggregated cells under higher magnification, these observations support previous reports of upregulation of integrins in the microgravity culture environment [Unsworth and Lelkes, 1998; Chang and Hughes-Fulford, 2009] and integrin clustering, thus providing indirect evidence of focal adhesion complexes [Hynes, 2002; Arnaout et al., 2007].

Discussion

In this study, we have shown that microgravity cultures may afford specific advantages to support differentiation of cells through provision of three-dimensionality, low-shear fluid and reduced turbulence conditions [Hammond and Hammond, 2001; Navran, 2008; Mazzoleni et al., 2009]. Large aggregates of about 2–5 mm formed a shell of glycogen-positive viable cells circumscribing a core of eosinophilic cells, the latter observation, probably due to perturbed mass transport, and O_2 diffusion limitations. These spheroidal aggregates formed consistently and rapidly within 12–24 h. This contrasts with the 5-day culture period required to form hepatic spheroid cultures using spinner flasks or in ECM-hepatocyte growth factor (HGF) microarrays in unit gravity [Lazar et al., 1995b; Abu-Absi et al., 2002; Jones et al., 2009].

The above spheroids maintained characteristic morphological, ultrastructural and functional features of differentiated 3D hepatocyte cultures throughout the predetermined 12-day culture period. The presence of albumin was confirmed in microgravity cultures on days 6 and 12 by dot blot analysis (fig. 4d). Khaoustov et al. [1999] observed similar histological and ultrastructural characteristics of primary human hepatocytes cultured in a HARV microgravity environment which retained hepatic tissue-like structures and albumin mRNA expression for up to 60 days. In addition, we observed a high level of hepatic structural polarity as evidenced by domain-specific functional bile-canalicular and integrin α_5 expression. Assuming an average diameter of 25 μm for a 'spherical' PPH and cell compaction in a 5-mm-diameter spherical aggregate as evidenced histologically, the total number of cells per spheroid may be up to 8×10^6, with about 4×10^5 viable cells. Thus, such spheroid cultures, without exogenous biomatrix, contained a viable cell population perhaps several orders of magnitude greater than is observed using standard spheroid culture modalities. In contrast, spheroid formation in unit gravity achieves a range of spheroid sizes of only 50–160 μm in diameter, containing ≈100 viable cells throughout the 3D structure [Lazar et al., 1995a].

Viability and differentiated function of the hepatic spheroids was demonstrated by evidence of vital staining, cell polarity and the ability of these cells to metabolize the fluorescent bile acid analogue FDA as well as albumin production. AO/EtBr fluorescent staining of day-12-RCCS-HARV-cultured aggregates (fig. 4a) confirmed viability of the outer layer of PAS-positive cells (fig. 2a, 3a). Intracellular esterases cleave FDA to fluorescein only in viable cells, and FDA metabolism was demonstrated in day-12 spheroids (fig. 4b) by the intense green fluorescent staining of the apical (bile canalicular) domain, although it was difficult to distinguish individual cells in the multicellular aggregate fragment. In addition, the high viability of aggregates from the RCCS-HARV at day 12 was demonstrated by attachment onto uncoated TCP and subsequent formation of hepatocyte monolayers radiating from the cell aggregate base (fig. 4c). Albumin synthesis was also confirmed by immunodetection shown in figure 4d.

Although hepatocytes are regarded as fragile, attachment-dependent parenchymal cells, we have previously shown [Nelson et al., 2000] that PPHs readily attach to TCP with high plating efficiency, viability and functionality in serum-free, chemically defined media without exogenous matrix proteins, suggesting that PPHs (and/or the NPC fraction) can synthesize ECM components, in-

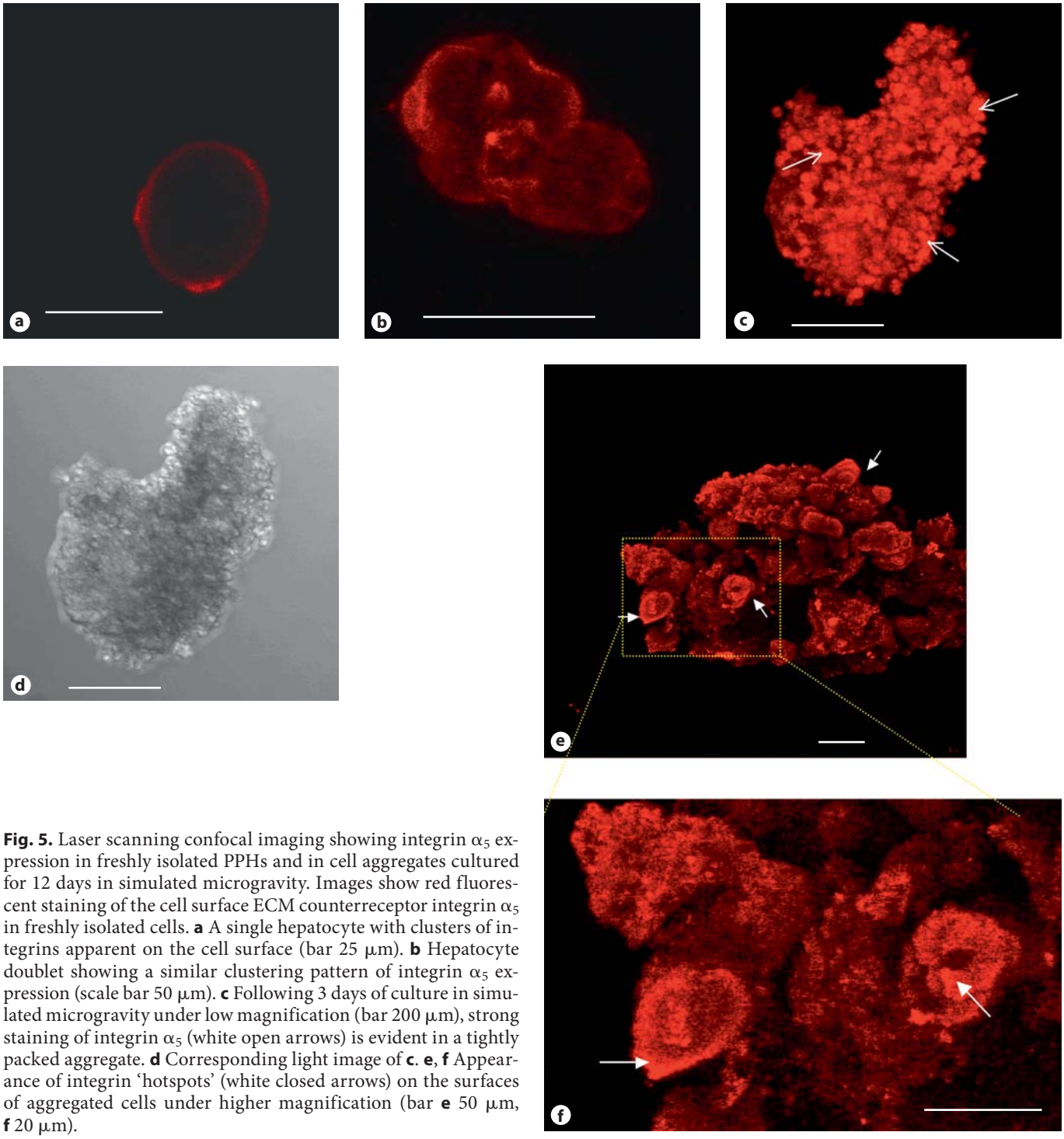

Fig. 5. Laser scanning confocal imaging showing integrin α_5 expression in freshly isolated PPHs and in cell aggregates cultured for 12 days in simulated microgravity. Images show red fluorescent staining of the cell surface ECM counterreceptor integrin α_5 in freshly isolated cells. **a** A single hepatocyte with clusters of integrins apparent on the cell surface (bar 25 μm). **b** Hepatocyte doublet showing a similar clustering pattern of integrin α_5 expression (scale bar 50 μm). **c** Following 3 days of culture in simulated microgravity under low magnification (bar 200 μm), strong staining of integrin α_5 (white open arrows) is evident in a tightly packed aggregate. **d** Corresponding light image of **c**. **e**, **f** Appearance of integrin 'hotspots' (white closed arrows) on the surfaces of aggregated cells under higher magnification (bar **e** 50 μm, **f** 20 μm).

cluding fibronectin, locally. In fact, rat and human hepatocytes, which have an absolute requirement for exogenous matrix proteins for attachment, can synthesize and secrete cellular fibronectin in vitro [Christiansen et al., 1988; Odenthal et al., 1992].

Hepatocytes can also be stabilized in vitro by integrin ligation resulting in upregulation of integrin $\alpha_5\beta_1$, which promotes survival and retention of liver-specific functions in heterotypic cocultures [Liu Tsang et al., 2007]. The day-12 viable cell population in the 3D microgravity

environment (but not 2D monolayer cultures on TCP; not shown) retains strong expression of this integrin class. In support of these data, active integrins are shown to be polarized at cellular surfaces [Giannelli et al., 2002] and typically cluster in the plane of the membrane [Hynes, 2002]. Although the mechanisms responsible for cellular self-assembly remain to be established, recent microarray studies show upregulation and stabilization of cell adhesion molecules in spheroid cultures of both HepG2 cells in microgravity [Chang and Hughes-Fulford, 2009] and rat hepatocyte spheroids in a novel 'rocker dish' format [Brophy et al., 2009]. We hypothesized that expression of integrin α_5 is important for preferential aggregation in microgravity cultures since it is intimately involved in the coordinated control – in concert with various ECM components and growth factors (including endothelial growth factor, EGF) – of cell shape and polarity, growth, movement and survival, important for the establishment and maintenance of differentiated function and tissue architecture [Giancotti and Ruoslahti, 1999].

Stable integrin expression on day-12 cells may be a result of the presence of fibronectin, associated with the modular $\alpha_5\beta_1$ heterodimer, which is produced by NPCs. Indeed, hepatocyte cultures on Matrigel, a matrix composed mostly of laminin, continued to lose expression of the integrin α_5 subunit over 7 days [Liu Tsang et al., 2007], although α_5 expression in this study was retained best in NPC coculture > double gel > Matrigel. The latter finding may be explained by the fact that hepatocytes cultured on Matrigel in unit gravity form spheroids with increased cell-cell interactions and decreased cell-matrix interactions. We have observed [Nelson et al., 2000] that, unlike single-cell rat or human hepatocyte isolates, PPHs naturally form small clusters of 5–20 cells even after comprehensive collagenase digestion of the liver matrix. Intuitively, this property of PPHs might be a beneficial attribute for the formation and study of 3D spheroid cultures. Maintenance of such cell-cell/cell-matrix contacts, as occurs in spheroid cultures, may well contribute to the enhanced differentiated cell function observed [Bhatia et al., 1998a, b, 1999].

Given the initial hepatic coculture seeding density of cells into the HARV was 1–5% NPCs (~95% hepatocytes), it is most likely that fibroblasts present in this fraction could secrete fibronectin, collagen and other ECM components. Thus, heterotypic cocultures may both induce liver-specific functions and preserve functional integrin expression. Further studies are required for identification of the presence of fibronectin or other components of the ECM, and a systematic assessment of the precise ratio of parenchymal:NPCs, which may optimize phenotypic and functional stability in microgravity cultures.

In our study, expression of the integrin α_5 subunit was observed in freshly isolated PPHs and up to day 12 in microgravity spheroid cultures (fig. 5). In contrast, the α_5-subunit was not expressed in 2D flattened monolayer cultures (not shown), whereas rat hepatocytes rapidly (<24 h) lose α_5-expression in unit gravity [Liu Tsang et al., 2007]. Spheroid formation in hepatoma cells [Lin and Chang, 2008] or rat primary hepatocytes both in 2D/3D culture formats [Tzanakakis et al., 2001] is characterized as: (1) formation of loose aggregates via integrin-ECM, (2) lag phase of cadherin expression, and (3) spheroid compaction via cadherin-based cell-cell interaction. In concordance with Robinson et al. [2004], it is mechanistically possible that an initial step in the formation of 3D spheroids in microgravity is spontaneous cell aggregation (enhanced by spatial colocation) followed by cell rearrangement (extensive cell-cell contacts; fig. 2b, c), and integrin α_5/fibronectin-dependent aggregate compaction (see SEM; fig. 3b, c), resulting in enhanced cellular/organoid cohesion. Indeed, figure 3c shows that some of the spheroid surface cells are flat, indicating that they strongly adhere to the cells around and beneath them.

Consistent with this notion is the observation that cells within the spheroid shell retain ultrastructural features of polarized hepatocytes including the presence of functional bile canaliculus-like channels (capable of FDA metabolism; fig. 4b) with characteristic microvillous processes delimited by tight junctions (fig. 2e, 3d). Figure 2 shows round nuclei/ nucleoli, with abundant mitochondria, granular endoplasmic reticulum and glycogen particles, features indicative of differentiated, in-vivo-like polarized hepatocytes. These findings are in agreement with previous morphological and differentiated functional data on rat hepatocyte spheroid formation supporting cellular polarization of the hepatocyte into apical and basolateral domains demonstrating structural and functional bile canaliculi [Yumoto et al., 1996; Abu-Absi et al., 2002]. This is considered important for the reemergence of differentiated phenotype and functions in vitro and is reflected by differences in gene expression patterns in PPH spheroids [Narayanan et al., 2002]. Moreover, the presence of integrin 'hotspots' (fig. 5e) may suggest focal adhesion kinase activation in response to integrin clustering induced by cell adhesion. In turn, focal adhesions are dynamic actin-integrin links forming part of a 'mechanosensing' molecular module [Ingber, 1999, 2006; Geiger et al., 2009].

We and others [Lazar, 1995a, b; Khaoustov et al., 1999; Jones et al., 2009; Tzanakakis et al., 2001] used serum-free chemically defined medium containing EGF and/or HGF (with potent mitogen and motogenic acitivity), insulin and dexamethasone. Studies have demonstrated that these were essential supplements for successful formation of floating rat hepatocyte spheroid cultures [Kawaguchi et al., 1992]. Furthermore, Michalopoulos et al. [2001] showed that isolated hepatocytes and NPCs in collagen-coated roller bottle cultures formed hepatic tissue constructs with structured histological formations and phenotypic maturation, bearing resemblance to characteristic hepatic histological organization only in the presence of HGF, EGF and dexamethasone. In contrast, spheroid formation is inhibited in the presence of serum [Hsiao et al., 1999; Abu-Absi et al., 2004]. Recently, Kidambi et al. [2009] demonstrated that serum has a predominantly negative effect on the metabolic function of primary rat and human hepatocytes. We therefore used the synthetic L-EGF (Sigma) in defined culture medium since it promotes cellular proliferation, differentiation and survival, and is a potent analogue of endogenous EGF. Using serum-free chemically defined medium, we have previously demonstrated sustained metabolic activity of microgravity-cultured cells for a predetermined period of 21 days [Dabos et al., 2001].

As viable spheroid shells are only <200 μm across, their culture in microgravity bears some caveats. Mass transfer constraints are a common problem with growing 3D spheroid cultures, whereby diffusion kinetics of oxygen and other nutrients is limited to <200 μm across multi-cell layers. However, the quality of microgravity cultures could further be enhanced by the use of a non-toxic biodegradable synthetic polymer scaffold, resulting in more efficient cell assembly and larger, morphologically and physiological more accurate viable cell aggregates. Indeed, scaffolding is considered to be a critical component in tissue engineering since it provides 3D cues for cell seeding, migration, growth and morphogenesis [Sundback and Vacanti, 2000].

Conclusions

This study has shown that in the absence of exogenous biomatrix scaffolding, PPHs cultured in chemically defined medium in microgravity rapidly form macroscopic 3D spheroid structures which exhibit ultrastructural, morphological and functional features of differentiated, polarized hepatic tissue. The low fluid shear environment may promote such attributes and offer advantages over spheroids cultured in conventional formats in unit gravity. Future studies are required to address the inherent limits of nutrient diffusion observed in the shell/core structures including delineation of the optimal conditions to enhance directed tissue self-assembly. Such tissue-engineering approaches may include: (1) vascularization, with appropriate levels of sinusoidal endothelial cells and angiogenic factors; (2) functionalized biodegradable scaffolds, e.g. designer peptide nanofibre scaffold [Gelain et al., 2007]; (3) appropriate oxygenation, cell-seeding density, heterotypic coculture ratios and interactions, hepatotrophic and matrix component(s), and (4) enhancement of the 'excluded volume effect' [Lareu et al., 2007], potentially advantageous in the closed-system RCCS-HARV, whereby polymeric macromolecules (e.g. 500-kDa dextran sulphate) essentially exclude aqueous volume, so increasing 'macromolecular crowding', thus accelerating enzymatic matrix production. Ultimately, success in this endeavour would result in assembly of high-fidelity hepatic tissue constructs capable of downstream applications in organ printing [Mironov et al., 2009], regenerative medicine and as a physiologically relevant 3D model system for drug metabolism, screening and toxicity studies.

Acknowledgements

This study was funded internally, from departmental funds of the Liver Laboratory Department of Hepatology, University of Edinburgh.

References

Abu-Absi, S.F., J.R. Friend, L.K. Hansen, W.S. Hu (2002) Structural polarity and functional bile canaliculi in rat hepatocyte spheroids. Exp Cell Res *274:* 56–67.

Abu-Absi, S.F., L.K. Hansen, W.S. Hu (2004) Three-dimensional co-culture of hepatocytes and stellate cells. Cytotechnology *45:* 125–140.

Arnaout, M.A., S. Goodman, J.P. Xiong (2007) Structure and mechanics of integrin-based cell adhesion. Curr Opin Cell Biol *19:* 495–507.

Auth, M.K.H., A. Ichihara (1998) Hepatocyte coculture, three-dimensional culture models and the extracellular matrix; in Strain, A.J., Diehl, A.M. (eds): Liver Growth and Repair, ed 1. London, Chapman & Hall, pp 465–481.

Becker, J.L., T.L. Prewett, G.F. Spaulding, T.J. Goodwin (1993) Three-dimensional growth and differentiation of ovarian tumor cell line in high aspect rotating-wall vessel: morphologic and embryologic considerations. J Cell Biochem *51:* 283–289.

Berthiaume, F., P.V. Moghe, M. Toner, M.L. Yarmush (1996) Effect of extracellular matrix topology on cell structure, function, and physiological responsiveness: hepatocytes cultured in a sandwich configuration. FASEB J *10:* 1471–1484.

Bhatia, S.N., U.J. Balis, M.L. Yarmush, M. Toner (1998a) Microfabrication of hepatocyte/fibroblast co-cultures: role of homotypic cell interactions. Biotechnol Prog *14:* 378–387.

Bhatia, S.N., U.J. Balis, M.L. Yarmush, M. Toner (1998b) Probing heterotypic cell interactions: hepatocyte function in microfabricated co-cultures. J Biomater Sci Polym Ed *9:* 1137–1160.

Bhatia, S.N., U.J. Balis, M.L. Yarmush, M. Toner (1999) Effect of cell-cell interactions in preservation of cellular phenotype: cocultivation of hepatocytes and nonparenchymal cells. FASEB J *13:* 1883–1900.

Botta, G.P., P. Manley, S. Miller, P.I. Lelkes (2006) Real-time assessment of three-dimensional cell aggregation in rotating wall vessel bioreactors in vitro. Nat Protoc *1:* 2116–2127.

Brophy, C.M., J.L. Luebke-Wheeler, B.P. Amiot, H. Khan, R.P. Remmel, P. Rinaldo, S.L. Nyberg (2009) Rat hepatocyte spheroids formed by rocked technique maintain differentiated hepatocyte gene expression and function. Hepatology *49:* 578–86.

Chang, T.T., M. Hughes-Fulford (2009) Monolayer and spheroid culture of human liver hepatocellular carcinoma cell line cells demonstrate distinct global gene expression patterns and functional phenotypes. Tissue Eng Part A *15:* 559–567.

Christiansen, B.S., J. Ingerslev, L. Heickendorff, C.M. Petersen (1988) Human hepatocytes in culture synthesize and secrete fibronectin. Scand J Clin Lab Invest *48:* 685–690.

Couvelard, A. (1998) Expression of integrins during liver organogenesis in humans. Hepatology *27:* 839–847.

Curcio, E., S. Salerno, G. Barbieri, L. De Bartolo, E. Drioli, A. Bader (2007) Mass transfer and metabolic reactions in hepatocyte spheroids cultured in rotating wall gas-permeable membrane system. Biomaterials *28:* 5487–5497.

Dabos, KJ, L.J. Nelson, T.J. Bradnock, J.A. Parkinson, I.H. Sadler, P.C. Hayes, J.N. Plevris (2001) The simulated microgravity environment maintains key metabolic functions and promotes aggregation of primary porcine hepatocytes. Biochim Biophys Acta *1526:* 119–130.

Decaens, C., M. Durand, B. Grosse, D. Cassio (2008) Which in vitro models could be best used to study hepatocyte polarity? Biol Cell *100:* 387–98.

Feder-Mengus, C., S. Ghosh, A. Reschner, I. Martin, G.C. Spagnoli (2008) New dimensions in tumor immunology: what does 3D culture reveal? Trends Mol Med *14:* 333–340.

Geiger, B., J.P. Spatz, A.D. Bershadsky (2009) Environmental sensing through focal adhesions. Nat Rev Mol Cell Biol *10:* 21–33.

Gelain, F., A. Horii, S. Zhang (2007) Designer self-assembling peptide scaffolds for 3-D tissue cell cultures and regenerative medicine. Macromol Biosci *7:* 544–551.

Giancotti, F.G., E. Ruoslahti (1999) Integrin signaling. Science *285:* 1028–1032.

Giannelli, G., E. Fransvea, F. Marinosci, C. Bergamini, S. Colucci, O. Schiraldi, S. Antonaci (2002) Transforming growth factor-1 triggers hepatocellular carcinoma invasiveness via $\alpha_3\beta_1$ integrin. Am J Pathol *161:* 183–193.

Gkretsi, V., W.C. Bowen, Y. Yang, C. Wu, G.K. Michalopoulos (2007) Integrin-linked kinase is involved in matrix-induced hepatocyte differentiation. Biochem Biophys Res Commun *353:* 638–643.

Godoy, P., J.G. Hengstler, I. Ilkavets, C. Meyer, A. Bachmann, A. Müller, G. Tuschl, S.O. Mueller, S. Dooley (2009) Extracellular matrix modulates sensitivity of hepatocytes to fibroblastoid dedifferentiation and transforming growth factor β-induced apoptosis. Hepatology *49:* 2031–2043.

Goodwin, T.J., T.L. Prewett, D.A. Wolf, G.F. Spaulding (1993) Reduced shear stress: a major component in the ability of mammalian tissues to form three-dimensional assemblies in simulated microgravity. J Cell Biochem *51:* 301–311.

Griffith, L.G., M.A. Swartz (2006) Capturing complex 3D tissue physiology in vitro. Nat Rev Mol Cell Biol *7:* 211–224.

Hammond, T.G., J.M. Hammond (2001) Optimized suspension culture: the rotating-wall vessel. Am J Physiol Renal Physiol *281:* F12–F25.

Holly, S.P., M.K. Larson, L.V. Parise (2000) Multiple roles of integrins in cell motility. Exp Cell Res *261:* 69–74.

Hsiao, C.C., J.R. Wu, F.J. Wu, W.J. Ko, R.P. Remmel, W.S. Hu (1999) Receding cytochrome P450 activity in disassembling hepatocyte spheroids. Tissue Eng *5:* 207–221.

Hynes, R.O. (2002) Integrins: bidirectional, allosteric signaling machines. Cell *110:* 673–687.

Ingber, D. (1999) How cells (might) sense microgravity. FASEB J *13(suppl):* S3–S15.

Ingber, D.E. (2006) Cellular mechanotransduction: putting all the pieces together again. FASEB J *20:* 811– 827.

Jauregui, H.O., H. Naik, S. Santangini, D.M. Trenkler, C.J.P. Mullon (1997) The use of microcarrier-roller bottle culture for large-scale production of porcine hepatocytes. Tissue Eng *3:* 17–25.

Jessup, J.M., T.J. Goodwin, G. Spaulding (1993) Prospects for use of microgravity-based bioreactors to study three-dimensional host-tumor interactions in human neoplasia. J Cell Biochem *51:* 290–300.

Jones, C.N., N. Tuleuova, J.Y. Lee, E. Ramanculov, A.H. Reddi, M.A. Zern, A. Revzin (2009) Cultivating liver cells on printed arrays of hepatocyte growth factor. Biomaterials *30:* 3733–3741.

Kawaguchi, M., N. Koide, K. Sakaguchi, T. Shinji, T. Tsuji (1992) Combination of epidermal growth factor and insulin is required for multicellular spheroid formation of rat hepatocytes in primary culture. Acta Med Okayama *46:* 195–201.

Khaoustov, V.I., G.J. Darlington, H.E. Soriano, B. Krishnan, D. Risin, N.R. Pellis, B. Yoffe (1999) Induction of three-dimensional assembly of human liver cells by simulated microgravity. In Vitro Cell Dev Biol Anim *35:* 501–509.

Kidambi, S., R.S. Yarmush, E. Novik, P. Chao, M.L. Yarmush, Y. Nahmias (2009) Oxygen-mediated enhancement of primary hepatocyte metabolism, functional polarization, gene expression, and drug clearance. Proc Natl Acad Sci USA *106:* 15714–15719.

Kim, B.-S., D.J. Mooney (1998) Development of biocompatible synthetic extracellular matrices for tissue engineering. TIBTECH *16:* 224–230.

Kwon, O., S.B. Devarakonda, J.M. Sankovic, R.K. Banerjee (2008) Oxygen transport and consumption by suspended cells in microgravity: a multiphase analysis. Biotechnol Bioeng *99:* 99–107.

Lareu, R.R., K.H. Subramhanya, Y. Peng, P. Benny, C. Chen, Z. Wang, R. Rajagopalan, M. Raghunath (2007) Collagen matrix deposition is dramatically enhanced in vitro when crowded with charged macromolecules: the biological relevance of the excluded volume effect. FEBS Lett *581:* 2709–2714.

Larsen, M., V.V. Artym, J.A. Green, K.M. Yamada (2006) The matrix reorganized: extracellular matrix remodeling and integrin signaling. Curr Opin Cell Biol *18:* 463–471.

Lazar, A., H.J. Mann, R.P. Remmel, R.A. Shatford, F.B. Cerra, W.S. Hu (1995a) Extended liver-specific functions of porcine hepatocyte spheroids entrapped in collagen gel. In Vitro Cell Dev Biol Anim *31:* 340–346.

Lazar, A., M.V. Peshwa, F.J. Wu, C.M. Chi, F.B. Cerra, W.S. Hu (1995b) Formation of porcine hepatocyte spheroids for use in a bioartificial liver. Cell Transplant *4:* 259–268.

Lin, R.Z., H.Y. Chang (2008) Recent advances in three-dimensional multicellular spheroid culture for biomedical research. Biotechnol J *3:* 1172–1184.

Liu Tsang, V., A.A. Chen, L.M. Cho, K.D. Jadin, R.L. Sah, S. DeLong, J.L. West, S.N. Bhatia (2007) Fabrication of 3D hepatic tissues by additive photopatterning of cellular hydrogels. FASEB J *21:* 790–801.

Martin, Y., P. Vermette (2005) Bioreactors for tissue mass culture: design, characterization, and recent advances. Biomaterials *26:* 7481–7503.

Mazzoleni, G., D. Di Lorenzo, N. Steimberg (2009) Modelling tissues in 3D: the next future of pharmaco-toxicology and food research? Genes Nutr *4:* 13–22.

Michalopoulos, G.K., W.C. Bowen, K. Mulè, D.B. Stolz (2001) Histological organization in hepatocyte organoid cultures. Am J Pathol *159:* 1877–1887.

Michalopoulos, G.K., W.C. Bowen, V.F. Zajac, D. Beer-Stolz, S. Watkins, V. Kostrubsky, S.C. Strom (1999) Morphogenetic events in mixed cultures of rat hepatocytes and nonparenchymal cells maintained in biological matrices in the presence of hepatocyte growth factor and epidermal growth factor. Hepatology *29:* 90–100.

Mironov, V., R.P. Visconti, V. Kasyanov, G. Forgacs, C.J. Drake, R.R. Markwald (2009) Organ printing: tissue spheroids as building blocks. Biomaterials *30:* 2164–2174.

Mitaka, T., F. Sato, T. Mizuguchi, T. Yokono, Y. Mochizuki (1999) Reconstruction of hepatic organoid by rat small hepatocytes and hepatic nonparenchymal cells. Hepatology *29:* 111–125.

Moghe, P.V., R.N. Coger, M. Toner, M. Yarmush (1997) Cell-cell interactions are essential for maintenance of hepatocyte function in collagen gel but not on matrigel. Biotech Bioeng *56:* 706–711.

Nahmias, Y., F. Berthiaume, M.L. Yarmush (2007) Integration of technologies for hepatic tissue engineering. Adv Biochem Eng Biotechnol *103:* 309–329.

Narayanan, R.A., A. Rink, C.W. Beattie, W.S. Hu (2002) Differential gene expression analysis during porcine hepatocyte spheroid formation. Mamm Genome *13:* 515–523.

Navran, S. (2008) The application of low shear modeled microgravity to 3-D cell biology and tissue engineering. Biotechnol Annu Rev *14:* 275–296.

Nelson, L.J., P.N. Newsome, A.F. Howie, P.W. Hadoke, K.J. Dabos, S.W. Walker, P.C. Hayes, J.N. Plevris (2000) An improved ex vivo method of primary porcine hepatocyte isolation for use in bioartificial liver systems. Eur J Gastroenterol Hepatol *12:* 923–930.

Nyberg, S.L., K. Shirabe, M.V. Peshwa, T.D. Sielaff, P.L. Crotty, H.J. Mann, R.P. Remmel, W.D. Payne, W.S. Hu, F.B. Cerra (1993) Extracorporeal application of a gel-entrapment, bioartificial liver: demonstration of drug metabolism and other biochemical functions. Cell Transplant *2:* 441–452.

Odenthal, M., K. Neubauer, F.E. Baralle, H. Peters, K.H. Meyer zum Buschenfelde, G. Ramadori (1992) Rat hepatocytes in primary culture synthesize and secrete cellular fibronectin. Exp Cell Res *203:* 289–296.

Parsons-Wingerter, P.A., W.M. Saltzman (1993) Growth versus function in the three-dimensional culture of single and aggregated hepatocytes within collagen gels. Biotechnol Prog *9:* 600–607.

Peshwa, M.V., F.J. Wu, H.L. Sharp, F.B. Cerra, W.S. Hu (1996) Mechanistics of formation and ultrastructural evaluation of hepatocyte spheroids. In Vitro Cell Dev Biol Anim *32:* 197–203.

Robinson, E.E., Foty R.A., Corbett S.A. (2004) Fibronectin matrix assembly regulates $\alpha_5\beta_1$-mediated cell cohesion. Mol Biol Cell *15:* 973–981.

Spaulding, G.F., J.M. Jessup, T.J. Goodwin (1993) Advances in cellular construction. J Cell Biochem *51:* 249—251

Stamatoglou, S.C., R.C. Hughes (1994) Cell adhesion molecules in liver function and pattern formation. FASEB J *8:* 420–427.

Stamatoglou, S.C., K.H. Sullivan, S. Johansson, P.M. Bayley, I.D. Burdett, R.C. Hughes (1990) Localization of two fibronectin-binding glycoproteins in rat liver and primary hepatocytes. Co-distribution in vitro of integrin ($\alpha_5\beta_1$) and non-integrin (AGp110) receptors in cell-substratum adhesion sites. J Cell Sci *97(pt 4):* 595–606.

Sundback, C.A., J.P. Vacanti (2000) Alternatives to liver transplantation: from hepatocyte transplantation to tissue-engineered organs. Gastroenterology *118:* 438–442. Review.

Théry, M., V. Racine, M. Piel, A. Pépin, A. Dimitrov, Y. Chen, J.B. Sibarita, M. Bornens (2006) Anisotropy of cell adhesive microenvironment governs cell internal organization and orientation of polarity. Proc Natl Acad Sci USA *103:* 19771–19776.

Tuschl, G., J. Hrach, Y. Walter, P.G. Hewitt, S.O. Mueller (2009) Serum-free collagen sandwich cultures of adult rat hepatocytes maintain liver-like properties long term: a valuable model for in vitro toxicity and drug-drug interaction studies. Chem Biol Interact *181:* 124–137.

Tzanakakis, E.S., K. Hansen, W.-S. Hu (2001) The role of actin filaments and microtubules in hepatocyte spheroid self-assembly. Cell Motil Cytoskelt *48:* 175–189.

Unsworth, B.R., P.I. Lelkes (1998) Growing tissues in microgravity. Nature Medicine *4:* 901–907.

Yamada, K.M., E. Cukierman (2007) Modeling tissue morphogenesis and cancer in 3D. Cell *130:* 601–610.

Yumoto, A.U., S. Watanabe, M. Hirose, T. Kitamura, Y. Yamaguchi, N. Sato (1996) Structural and functional features of bile canaliculi in adult rat hepatocyte spheroids. Liver *16:* 61–66.